



Anatomical Characteristics and Taxonomic Significance of Rhizophoraceae Mangrove Leaves

I Made Saka Wijaya*, Luh Putu Eswaryanti Kusuma Yuni, Ni Kadek Rika Pramesti, I Wayan Bagus Kusuma Suarsana, Adi Ariyanto Wibisono

Udayana University, Indonesia

*Correspondence: E-mail: sakawijaya@unud.ac.id

ABSTRACT

Rhizophoraceae is a mangrove family that spread from landward to seaward zones and dominated Benoa Bay in Bali, Indonesia. Mangroves are already studied in many approaches but insufficient in anatomical approach. This research aims to determine the anatomical characteristics of Rhizophoraceae mangrove leaves in Benoa Bay, as well as determine the taxonomic significance. The research was conducted at four locations in Benoa Bay with four mangrove species: *Bruguiera gymnorhiza*, *Ceriops tagal*, *Rhizophora apiculata*, and *Rhizophora mucronata*. Leaf anatomical data was collected by using a modified free-hand section method to obtain leaf transversal structure and replica paradermal to obtain epidermal structure. The data analyzed descriptively and completed with a numerical taxonomy approach by dendrogram and principal component analysis (PCA). Mangrove leaves have general structures such as epidermis, palisade mesophyll, sponge mesophyll, vascular bundles, and stomata, as well as several typical structures such as hypodermis layer, calcium oxalate crystals, and sclereids. The results of the numerical taxonomic analysis revealed several characteristics with taxonomic significance were occurrence of astrosclereid, number of upper hypodermal layers, thickness ratio of hypodermal to lamina, thickness ratio of mesophyll palisade to sponges, thickness ratio of mesophyll sponges to lamina, and type of stomata.

© 2024 Tim Pengembang Jurnal UPI

ARTICLE INFO

Article History:

Submitted/Received 01 Jun 2024

First Revised 05 Jul 2024

Accepted 09 Sep 2024

First Available Online 10 Sep 2024

Publication Date 01 Dec 2024

Keyword:

Mangrove anatomy,
Numerical taxonomy,
Plasticity,
Stomata.

1. INTRODUCTION

Mangroves are plant communities that have morphological and physiological adaptations in a habitat that are influenced by sea tides. Mangroves are mainly distributed in tropical-subtropical regions, extending toward 30° in north and south latitudes (Giri et al., 2011). Ecologically, mangroves are a connecting ecosystem between land and ocean (Carugati et al., 2018) with many ecological functions, such as a spawning area, nursery ground, protecting juvenile phases of some fishes and crustaceans, pollutant filtration, protecting the coastline, and one of the excellent carbon sink areas (Kauffman et al., 2020; Romañach et al., 2018). Although provides many ecological functions, mangrove is an ecosystem that faces major anthropogenic disturbances, particularly the conversion of mangroves into ponds (intensive fishing) recognized as the main factor causing mangrove destruction and the decline in the world's mangrove forest area (Valiela et al., 2001; Thomas et al., 2017) and indirectly increases carbon emissions in the atmosphere (Adame et al., 2021).

With so much anthropogenic damage, mangroves not only have to adapt to natural fluctuations but also to human-derived environmental changes. The first stage of adaptation is a physiological response which over a certain period will change its structure. These physiological responses can be observed more clearly through an anatomical approach to solving how the variations relate to the species' fitness in an ecosystem (Strock et al., 2022). The anatomical characteristics are known as one of the significant characteristics in the taxonomical study (Hong et al., 2018; Filartiga et al., 2022), but the physiological responses tend to initiate the character plasticity that caused the taxonomic ambiguity. However, not all plant species have to develop such plastic characters. Some species have generalist anatomical characteristics with no significant changes even though the species grows in varied environments. Therefore, to increase data regarding the anatomical characteristics of mangroves, observations are needed on the anatomical structure of mangroves that live in varied environments, including environments that experience ecological disturbances.

Leaves are one of the plant organs that are sensitive to environmental changes because each mangrove species will form new leaves within a certain period according to environmental conditions. Concerning anatomy, the anatomical structure of mangrove leaves shows distinctive characteristics as a mechanism for physiological adaptation to environmental conditions in intertidal areas, especially adaptation to inundation and regulation of salt levels (Tatongjai et al., 2021). Mangrove genera such as *Avicennia* and *Aegiceras* have salt glands to excrete salt through the leaves (Tobing et al., 2022), while species without salt glands such as the Rhizophoraceae (*Rhizophora*, *Bruguiera*, and *Ceriops*) have roots that are capable of ultrafiltration to reduce salt levels (Vinoth et al., 2019). In Rhizophoraceae, the remaining salt is deposited on the leaves which are then shed when the leaves are old which is also found in the genus *Sonneratia*.

The fundamental research has been reported by Tihurua et al. (2023) which provides the leaf anatomical characteristics for some mangrove species in Indonesia. Related to the environment, the prior research reveals the leaf anatomical plasticity in mangroves that is influenced by salinity, such as in *Bruguiera parviflora* (Parida et al., 2004), *Rhizophora mangle* (Sánchez et al., 2021), *Sonneratia caseolaris* (Tatongjai et al., 2021), and *Avicennia marina* (Tobing et al., 2022). The environmental degradation due to heavy metal pollution also caused the anatomical alteration in mangrove leaves, such as in *A. marina* which shows quantitative variations in mesophyll tissue, hypodermis, and trichomes between the polluted area and the pristine area (Raju & Ramakrishna, 2021). The character plasticity is

also related to the growth phases of the species, which is the juvenile phase that tends to reflect more variations compared to the mature tree (Tatongjai *et al.*, 2021).

The larger area tends to provide diverse environmental variations that lead to the character plasticity. In Bali, the largest mangrove area is in the Ngurah Rai Forest Park located in Denpasar City and Badung Regency with 1,373.50 ha (Lugina *et al.*, 2017) dominantly located in Bena Bay. The mangrove in this area is in good condition but encounters ecological disturbances in several places such as stacked trash that affects the water quality. These piles of trash will cause changes in the characteristics of the mangroves that live in the area, one of which is the mangrove species from the Rhizophoraceae family. Mangrove species of the Rhizophoraceae family in Bena Bay consist of the *Bruguiera*, *Ceriops*, and *Rhizophora* genera which have varying salinity tolerances. Thus, they can be distributed from the landward to the seaward zone.

Much research has been carried out on mangroves in Bali, including on the mangrove community in Bena Bay. However, most of those research assesses the structure of mangrove communities (Andiani *et al.*, 2021; Dewi *et al.*, 2021), mangrove health index (Sugiana *et al.*, 2022), community comparison in natural and ex-fisheries areas (Wijaya *et al.*, 2023), floristic composition between island (Wijaya *et al.*, 2024), and others. Meanwhile, research on anatomical structures at the species level is very rarely carried out, in fact for the last 10 years there have been no research publications on mangrove anatomy in Bena Bay. On the other hand, mangrove anatomical research has been conducted in several provinces, such as Sulawesi (Tihuraa *et al.*, 2020, 2023), Maluku (Marantika *et al.*, 2021), and Java (Samiyarsih *et al.*, 2016; Tobing *et al.*, 2022).

Research on anatomical structures is one of the basic studies to see the ecophysiological impact of environmental conditions on species in that environment (Filartiga *et al.*, 2022; Sánchez *et al.*, 2021; Strock *et al.*, 2022). Changes in soil and water conditions due to ecological disturbance in Bena Bay will cause a physiological response, which will then influence the morphological and anatomical structure of the mangrove. The anatomical response will directly reflect the environmental status at a time. Thus, the scenario for climate change mitigation can be considered in advance (Sánchez *et al.*, 2021). To begin a study regarding this, this research aims to determine the anatomical characteristics of mangrove leaves of the Rhizophoraceae family in several environmental conditions in Bena Bay, as well as determine the taxonomic significance of this anatomical data.

2. METHODS

2.1. Study Site and Plant Materials

The research conducted in Bena Bay which divided into four sampling sites: (1) the pristine area of Batu Lumbang; (2) the trash-trap area; (3) the area with mixed trash in ex-fisheries area; and (4) the death mangrove area in Serangan. The locations for each sampling site are shown in the **Figure 1**. These four locations were chosen to study the variations in the anatomical structure of mangrove leaves in pristine and disturbed habitats.

The samples taken are mangrove species of the Rhizophoraceae family for each site. Thus, there were differences in mangrove species sampled as shown in **Table 1**. Four species of mangrove that were used were *Bruguiera gymnorhiza* (BG), *Ceriops tagal* (CT), *Rhizophora apiculata* (RA), and *Rhizophora mucronata* (RM). The species determination using three major identification books: Flora of Java Volume I, Field Guide of Mangrove in Indonesia, and Field Guide of Mangrove in Bali and Lombok. From four sampling sites, there were a total of 10 samples studied. The selection of species from the Rhizophoraceae family was based on the distribution of species that have tolerance in a wide range of mangrove

zonation in Bena Bay. BG and CT can be found in the landward zone to the middle zone, while RM and RA can spread from the landward zone to the middle zone, but in some circumstances also reach the seaward zones.

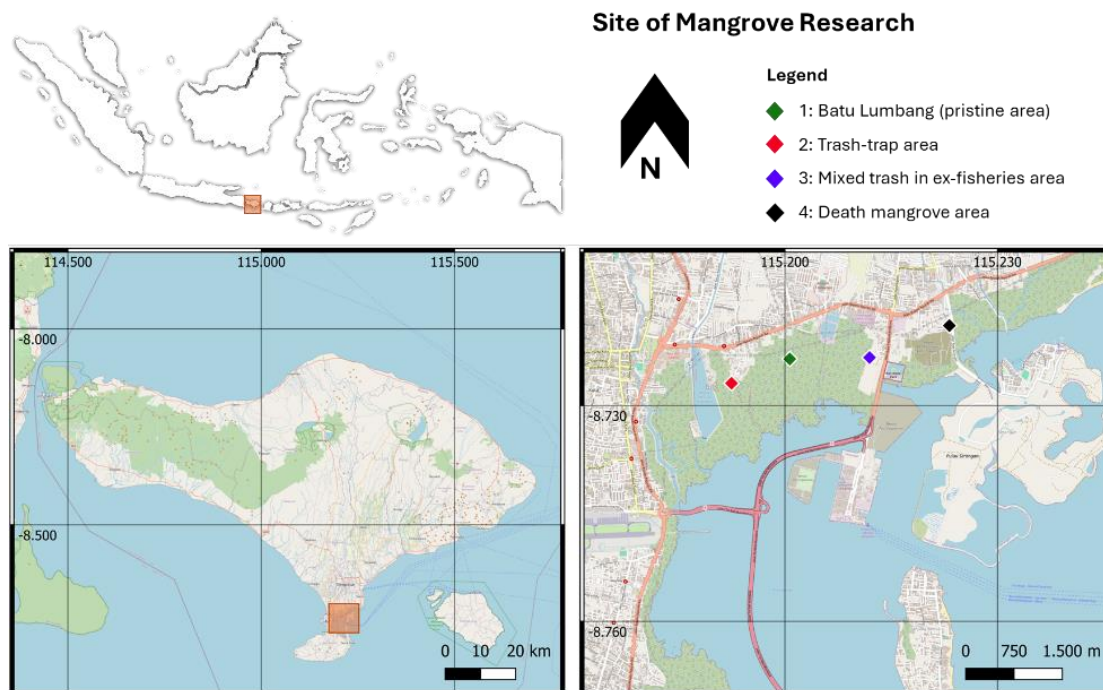


Figure 1. The study site of Rhizophoraceae mangrove sampling in Bena Bay, Bali – Indonesia.

Table 1. Mangrove species of Rhizophoraceae which were sampled in each sampling site.

No	Species	Sampling sites			
		1	2	3	4
1	<i>Bruguiera gymnorhiza</i> (BG)	●	●		●
2	<i>Ceriops tagal</i> (CT)	●			●
3	<i>Rhizophora apiculata</i> (RA)	●		●	
4	<i>Rhizophora mucronata</i> (RM)	●	●	●	

Annotations: ● = sample collected; (1) the pristine area of Batu Lumbang; (2) trash-trap area; (3) area with mixed trash in ex-fisheries area; and (4) death mangrove area in Serangan.

2.2. Anatomical Data Collection

The experiments were done in the following:

- (i) Sampling collection. Sampling was conducted in the study site according to **Table 1**. Three leaves were collected from three different individuals for each species (total samples with replications = 36). The samples were confirmed by identification books and the leaf comparison of the samples is shown in **Figure 2**. The summary of morphological leaf characteristics is: *B. gymnorhiza* has elliptic-oblong leaves, 14-16 × 5-7 cm, entire margin, acute apex, and cuneate or somewhat rounded at base; *C. tagal* has the smallest leaves with oval-obovate shape, 8-10 × 5-6 cm, entire margin, obtuse apex, and acute-cuneate at base; *R. apiculata* has elliptic-oblong or sometimes lanceolate leaves, 13-15 × 5-6 cm, entire margin, mucronate apex, cuneate-obtuse at base; and *R. mucronata* has broadly elliptic-oblong leaves, 15-23 × 8-12 cm, entire margin, mucronate apex, cuneate-obtuse at the base. *Rhizophora* leaf has a swirled tip. Thus, the apex looks like it has a tail. This trait can be used to differentiate the

leaves of *R. apiculata* from *B. gymnorhiza* which is difficult to distinguish. The leaves were purposively collected with criteria: (1) the leaves were mature and fully unfolding which usually at the third or fourth; (2) there was no trace of pest and disease; and (3) the tree was old enough with height more than 5 m to indicates the tree has been adapted to the environment of the study site. The leaves are then cleaned on the water to remove the remnant dirt and then dried by tissue to absorb the excess water. After drying, the leaves are then put into the sample bottle and filled with 70% alcohol.

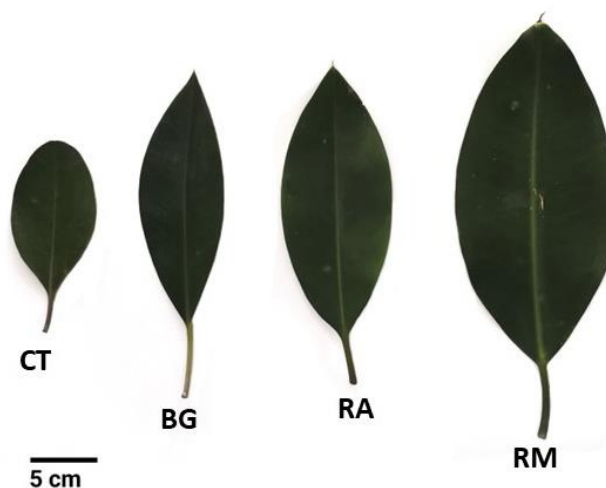


Figure 2. Leaf comparison of Rhizophoraceae mangrove in Benoa Bay. (Annotations: CT = *Ceriops tagal*; BG = *Bruguiera gymnorhiza*; RA = *Rhizophora apiculata*; RM = *Rhizophora mucronata*)

- (ii) Transversal section. The transversal section used the free-hand section method with some modifications in clearing solution (using 5% sodium hypochlorite) and staining solution (using 0.25% safranin and 1% fast green). The collected leaves were taken out of a bottle sample and then dried using a tissue to remove the alcohol from the surface of the leaves. The leaves were cut into smaller parts (1 x 1 cm) that consisted of a leaf midrib and lamina. The cut leaves are then inserted into the incision of the carrot which acts as supporting materials to 'embed' the cut leaves. The leaves-carrot then sliced as thinly as possible using a razor blade. The sample (sliced leaves) was then fixated in the FAA (formaldehyde – acetic acid – alcohol ethyl) for 10 minutes. Next, the sample was taken and soaked in 5% sodium hypochlorite for 2-5 minutes followed by immersion in 70% alcohol for 5 minutes. The sample was then stained in 0.25% safranin for 15 seconds. After staining, the sample was rinsed with 70% alcohol for 1 minute. After that, secondary staining was carried out with 1% fast green for 15 seconds, followed by rinsing using 70% alcohol for 15 seconds. The sample was mounted on the object glass with a drop of water and then closed with a cover glass. The microscopic observation using an Olympus CX-21 microscope equipped with Optilab, while image processing using Image Raster software. The characters observed were epidermal and hypodermal tissue, palisade, sponge mesophyll, vascular bundle, sclerenchyma tissue, and non-protoplasmic components such as calcium oxalate crystals. For quantitative characters such as the thickness of the epidermis, the thickness of the hypodermis, the thickness of the palisade mesophyll, the thickness of the sponge mesophyll, and the thickness of the leaves, we used 5 measurements for each replication to increase the precision.

- (iii) Replica paradermal. The collected leaves were taken out of a bottle sample and then dried using a tissue to remove the alcohol from the surface of the leaves. The mangrove leaves contain thick cuticles on the epidermal which can cause an unclear casting of the epidermal. To obtain a clearer replica, we improvised to remove the cuticle by immersing the leaves in the 5% sodium hypochlorite for 1 minute, then scrubbing both leaves' surfaces using a fine brush. The removed cuticle will be in the form of a dull-clear thin membrane. After removing the cuticle, the clear nail polish was applied on the lower surface (abaxial) of the leaves and then allowed to dry for 5-10 minutes. The clear tape or plaster is then attached to the dried nail polish. Thus, the cast epidermal on the nail polish will stick to the clear tape. The clear tape stuck to the object glass, and then the cast epidermal was observed through an Olympus CX-21 microscope equipped with Optilab. The image was then processed using Image Raster software. Since the species of Rhizophoraceae are hypostomatic, the stomata are only assessed for the lower surface (abaxial) of the leaf. The characters observed were epidermal cells, guard cells, and subsidiary cells. To obtain more data, the type of stomata was determined based on the arrangement of the subsidiary cells. The density of stomata and epidermal was calculated by counting the number of stomata or epidermal per mm^2 , while the index of stomata was calculated as a percentage by dividing the number of stomata by the total of cells (stomata + epidermal cells).

2.3. Data Analysis

Sampling The data obtained were analyzed descriptively to determine the anatomical differences in Rhizophoraceae mangrove leaves among species and various habitat types, and presented as pictures and tables. To study the taxonomic signification of the anatomical characteristics, a numerical taxonomic approach was carried out to determine the anatomical similarity of each species and continued with principal component analysis to determine their distinctive characteristics. The numerical taxonomy approach uses MVSP software with four main stages: (1) character determination and standardization for scoring; (2) creating a similarity matrix using the Gower's general coefficient algorithm; (3) dendrogram construction using the UPGMA (unweighted pair group method with arithmetic mean) algorithm; and (4) principal component analysis (PCA) in the form of a scatter plot. For numerical taxonomy analysis, all samples are known as operational taxonomical units (OTUs).

The character selection and scoring criteria are shown in **Table 2**, while the scores for each character in each OTU are shown in **Table 3**. Giving scores to each character is quite tricky. Thus, justification is needed as a basis for giving scores. In this study, simpler characters were given a lower value compared to more complex characters, for example, the K-1 character which gave a value of 0 for U-shaped vascular bundles and a value of 1 for vascular bundles that were rounded with U-shaped at the lower. Another note is on the character ratio for K-11 to K-14. The criteria provided do not correspond to the measurement results because they are standardized. In K-11 to K-14 interval standardization is carried out by subtracting the value for each species from the average value for each character. This aims to re-scoring and get the same zero average value. Furthermore, the score given to the 'new value' uses the same interval, namely 0.10 if the difference between the highest and lowest values is more than 0.25. If the difference is less than that (as in K-13), then use binary score, 0 if the 'new value' is equal or less than zero, and 1 if higher than zero.

Some characters that indicate plastic adaptation were analyzed using a mean comparison test in IBM SPSS-19 software. Seven characters that are compared within the species are K-11 (thickness ratio of hypodermal to lamina), K-12 (thickness ratio of mesophyll palisade to sponges), K-13 (thickness ratio of mesophyll palisade to lamina), K-14 (thickness ratio of mesophyll sponges to lamina), K-19 (index of stomata (IS)), K-20 (density of stomata (mm^{-2})), and K-21 (density of epidermal cells (mm^{-2})). Before the analysis began, the Shapiro–Wilk normality test was conducted. All the data did not show proportional normality. Thus, the data was analyzed using Mann-Whitney nonparametric analysis. In this analysis, if the value of asymp. Sig. (2-tailed) more than 0.050, the mean between the two groups is insignificantly different.

Table 2. The leaf anatomical characteristics of Rhizophoraceae mangrove that used in the numerical taxonomy approach.

Code	Characters	Score
Transversal section through the midrib		
K-1	Shapes of the vascular tissue	U-shaped (0); Rounded with U-shaped at the lower (1)
K-2	Number of upper hypodermal layer(s) in the midrib	2-3 layers (0); 5-7 layers (1); 6-8 layers (2)
K-3	Occurrence of mesophyll palisade above the vascular tissue	Absent (0); present (1)
K-4	Occurrence of sclereid (spheroidal) in vascular tissue	A small amount, sparsely at the outer of phloem in a very small cluster or one stack (0); moderate amount, sclereid clustering in 1-2 stacks (1); high amount, dense sclereid more than 2 stacks (2) RA: moderate amount (sclereid clustering in 1-2 stacks)
K-5	Occurrence of sclereid (rhizosclereid) in palisade	Absent (0); present (1) The rhizosclereid in the palisade of the midrib. The curved lamina around the midrib's vascular tissue was identified as the part of the midrib. Only the part with uniform shape/scale was classified as lamina.
K-6	Occurrence of sclereid (astrosclereid) in midrib parenchyma	Absent (0); small amount, less than 10 fragments (1); moderate, 10-20 fragments (2); high amount, more than 20 fragments (3) The calculation considers the presence of a small part of the sclereid. The majority of astrosclereids are in the form of ophiurosclereids with many irregular branches. Thus, sometimes the sclereids are big, and sometimes in tiny size. We calculate all of them.
Transversal section through the lamina		
K-7	Number of hypodermal layer(s) (upper)	1 layer (0); 2 layers (1); mostly 5 layers (2); mostly 6 layers (3)
K-8	Number of hypodermal layer(s) (lower)	1 layer (0); 2 layers (1)
K-9	Hypodermal (upper) gradation	Absent (0); present (1)
K-10	Overlapping hypodermal to palisade	Absent (0); present (1)
K-11	Thickness ratio of hypodermal to lamina	< -0.10 (0); -0.10-0.00 (1); 0.01-0.10 (2); > 0.10 (3)
K-12	Thickness ratio of mesophyll palisade to sponges	< -0.10 (0); -0.10-0.00 (1); 0.01-0.10 (2); > 0.10 (3)
K-13	Thickness ratio of mesophyll palisade to lamina	≤ 0.00 (0); > 0.00 (1)

Table 2 (Continue). The leaf anatomical characteristics of Rhizophoraceae mangrove that used in the numerical taxonomy approach.

Code	Characters	Score
K-14	Thickness ratio of mesophyll sponges to lamina	< -0.10 (0); -0.10-0.00 (1); 0.01-0.10 (2); > 0.10 (3)
K-15	Oxalate crystal in palisade	Absent (0); present (1)
K-16	Occurrence of sclereid (rhizosclereid) in palisade	Absent (0); present (1)
K-17	Occurrence of sclereid (astrosclereid) in sponges	Absent (0); present (1)
Replica paradermal		
K-18	Type of stomata	Anomocytic (0); tetracytic (1); cyclocytic (2)
K-19	Index of stomata (IS)	The average $\leq 4.00\%$ (0); 4.01-5.00% (1); 5.01-6.00% (2); > 6.00% (3)
K-20	Density of stomata (mm^{-2})	The $\leq 75,00$ (0); 75.01-100.00 (1); 100.01-125.00 (2); > 125.00 (3)
K-21	Density of epidermal cells (mm^{-2})	The ≤ 1500.00 (0); 1500.01-2000.00 (1); > 2000.00 (2)

Table 3. The score of leaf anatomical characteristics of Rhizophoraceae mangrove.

Code	BG-1	BG-2	BG-4	CT-1	CT-4	RA-1	RA-3	RM-1	RM-2	RM-3
K-1	0	0	0	1	1	1	1	1	1	1
K-2	0	0	0	0	0	2	2	1	1	1
K-3	0	0	0	1	1	0	0	0	0	0
K-4	0	0	0	1	2	1	1	1	0	1
K-5	0	0	0	0	0	1	1	1	1	1
K-6	0	0	0	0	0	1	1	2	3	3
K-7	0	0	0	1	1	3	3	2	2	2
K-8	0	0	0	1	1	0	0	0	0	0
K-9	0	0	0	0	0	1	1	1	1	1
K-10	0	0	0	0	0	1	1	1	1	1
K-11	0	0	0	0	0	3	3	3	3	3
K-12	1	0	0	0	0	2	3	1	3	1
K-13	1	0	1	0	0	0	0	0	0	0
K-14	3	3	2	3	3	0	0	0	0	1
K-15	1	1	1	1	1	0	0	0	0	0
K-16	0	0	0	0	0	0	1	1	1	1
K-17	0	0	0	0	0	1	1	1	1	1
K-18	1	1	1	2	2	0	0	0	0	0
K-19	3	2	2	1	0	0	0	1	3	2
K-20	2	3	2	0	0	1	1	1	2	0
K-21	1	1	1	1	2	2	2	1	0	0

3. RESULTS AND DISCUSSION

3.1. The Anatomical Characteristics of Rhizophoraceae Mangrove

The anatomical description contains the anatomical traits based on the three parts that were observed in this study: midrib, lamina, and stomata. In general, there are no differences within species, particularly the qualitative traits. The transversal section of the midrib is presented in **Figure 3**, while the lamina in **Figure 4**. For the replica paradermal or stomata, **Figure 5** shows the stomata with 10×10 magnification and **Figure 6** shows the illustration of the stomata to simplify the shape and the distribution of the guard cells,

subsidiary cells, and epidermal cells. All the observed and measured characters are included in **Table 4**.

Bruguiera gymnorhiza. **Midrib**: 1 layer of epidermal with thick cuticle; 2-3 hypodermal layer, square-rectangle cells, smaller at the center of the midrib; vascular tissue in U-shaped, parenchymal tissue at the center, small amount of spheroidal sclereid at the outer edge of phloem; palisade mesophyll discontinues above the vascular tissue; oxalate crystal distributed in the parenchymal tissue and phloem. **Lamina**: 1 layer of the epidermal layer, lower epidermal smaller than the upper; 1 layer of upper hypodermal and 1 layer of lower hypodermal; 2-3 layers of mesophyll palisade, slender-shaped; mesophyll sponge with air chamber, rounded-irregular cells; calcium oxalate crystal distributed in hypodermal, palisade, and sponge mesophyll. **Stomata**: only at the abaxial, tetracytic with the index of stomata $5.17 \pm 0.47 - 6.16 \pm 0.48$ %.

Ceriops tagal. **Midrib**: 1 layer of epidermal with thick cuticle; 2-3 hypodermal layer, square-polygonal cells, smaller at the center of the midrib; vascular tissue rounded with U-shaped at the lower, thin layer of parenchymal tissue at the center (between the rounded and U-shaped vascular tissue), moderate-high amount of spheroidal sclereid at the outer of phloem, palisade mesophyll continues above the vascular tissue; oxalate crystal distributed in the parenchymal tissue and phloem. **Lamina**: 1 layer of epidermal layer, lower epidermal smaller than the upper; 2 layers of rounded-polygonal upper hypodermal and 2 layers of square-rectangular lower hypodermal; 1-3 (mostly 2) layers of mesophyll palisade, slender-shaped; mesophyll sponge with small air chamber, rounded-irregular cells; calcium oxalate crystal distributed in hypodermal, palisade, and sponge mesophyll. **Stomata**: only at the abaxial, cyclocytic with the index of stomata $3.05 \pm 0.50 - 4.15 \pm 0.55$ %.

Rhizophora apiculata. **Midrib**: 1 layer of epidermal with thick cuticle; 6-8 hypodermal layer, square-polygonal cells, smaller at the center of the midrib; vascular tissue rounded with U-shaped at the lower, thin layer of parenchymal tissue at the center (between the rounded and U-shaped vascular tissue), moderate amount of spheroidal sclereid at the outer of phloem; palisade mesophyll discontinue above the vascular tissue, a very small amount of rhizosclereid; spongy parenchymal below the vascular tissue, small amount of astrosclereid; oxalate crystal distributed in the parenchymal tissue and phloem. **Lamina**: 1 layer of epidermal layer, lower epidermal smaller than the upper; 6-7 (mostly 6) layers of rectangular-polygonal upper hypodermal, size gradation of upper hypodermal, 1 layer of square-rectangular lower hypodermal; dense mesophyll palisade, some parts were overlapped with the lowest upper hypodermal, small amount (or absent) of rhizosclereid; mesophyll sponge with air chamber, rounded-irregular cells, occurrence of astrosclereid; calcium oxalate crystal distributed in hypodermal, palisade, and sponge mesophyll. **Stomata**: only at the abaxial, anomocytic with the index of stomata $3.69 \pm 0.22 - 3.98 \pm 0.34$ %.

Rhizophora mucronata. **Midrib**: 1 layer of epidermal with thick cuticle; 5-7 hypodermal layer, square-polygonal cells, smaller at the center of the midrib; vascular tissue rounded with U-shaped at the lower, thin layer of parenchymal tissue at the center (between the rounded and U-shaped vascular tissue), moderate amount of spheroidal sclereid at the outer of phloem; palisade mesophyll discontinue above the vascular tissue, a very small amount of rhizosclereid; spongy parenchymal below the vascular tissue, moderate-high amount of astrosclereid; oxalate crystal distributed in the parenchymal tissue and phloem. **Lamina**: 1 layer of epidermal layer, lower epidermal smaller than the upper; 5-6 (mostly 5) layer of rectangular-polygonal upper hypodermal, size gradation of upper hypodermal, 1 layer of square-rectangular lower hypodermal; dense mesophyll palisade, some parts were

overlapped with the lowest upper hypodermal, high amount of rhizosclereid; mesophyll sponge with air chamber, rounded-irregular cells, occurrence of astrosclereid; calcium oxalate crystal distributed in hypodermal, palisade, and sponge mesophyll. **Stomata:** only at the abaxial, anomocytic with the index of stomata $4.27 \pm 0.18 - 6.67 \pm 0.22 \%$.

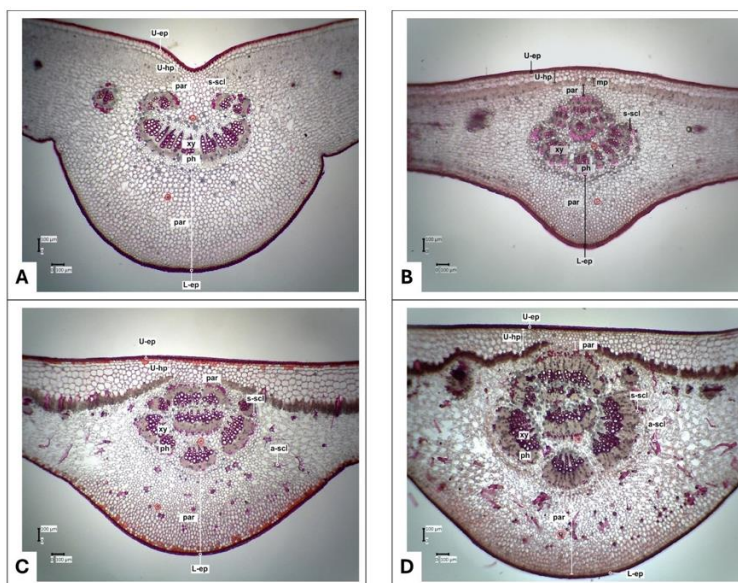


Figure 3. Transversal section of the leaf midrib of Rhizophoraceae mangrove in Benoa Bay with 10×10 magnification (A) *Bruguiera gymnorhiza*; (B) *Ceriops tagal*; (C) *Rhizophora apiculata*; and (D) *Rhizophora mucronata*. (Annotations: U-ep=upper epidermal; U-hp=upper hypodermal; par=parenchyma; mp= mesophyll palisade; xy=xylem; ph=phloem; s-scl=spheroidal sclereid; a-scl=astrosclereid; L-ep=lower epidermal; red circle=calcium oxalate crystal.)

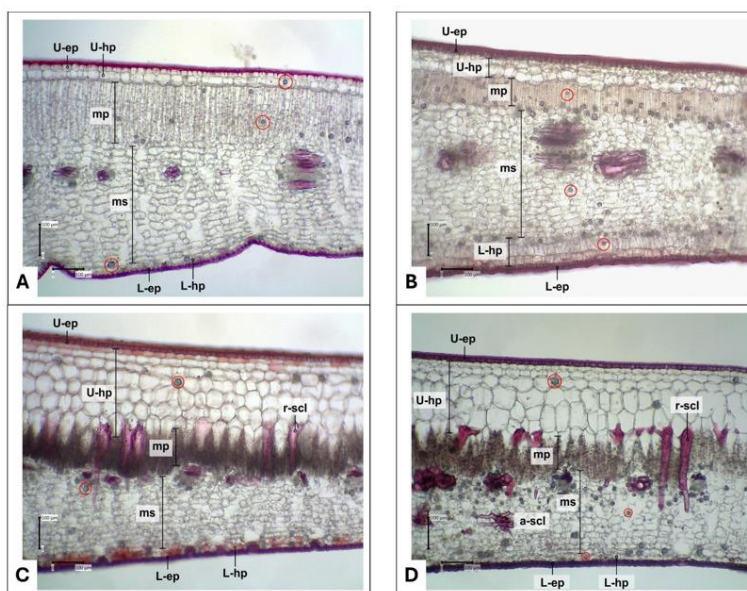


Figure 4. Transversal section of the leaf lamina of Rhizophoraceae mangrove in Benoa Bay with 10×10 magnification (A) *Bruguiera gymnorhiza*; (B) *Ceriops tagal*; (C) *Rhizophora apiculata*; and (D) *Rhizophora mucronata*. (Annotations: U-ep=upper epidermal; U-hp=upper hypodermal; mp= mesophyll palisade; ms=mesophyll sponge; r-scl=rhizosclereid; a-scl=astrosclereid; L-hp=lower hypodermal; L-ep=lower epidermal; red circle=calcium oxalate crystal.)

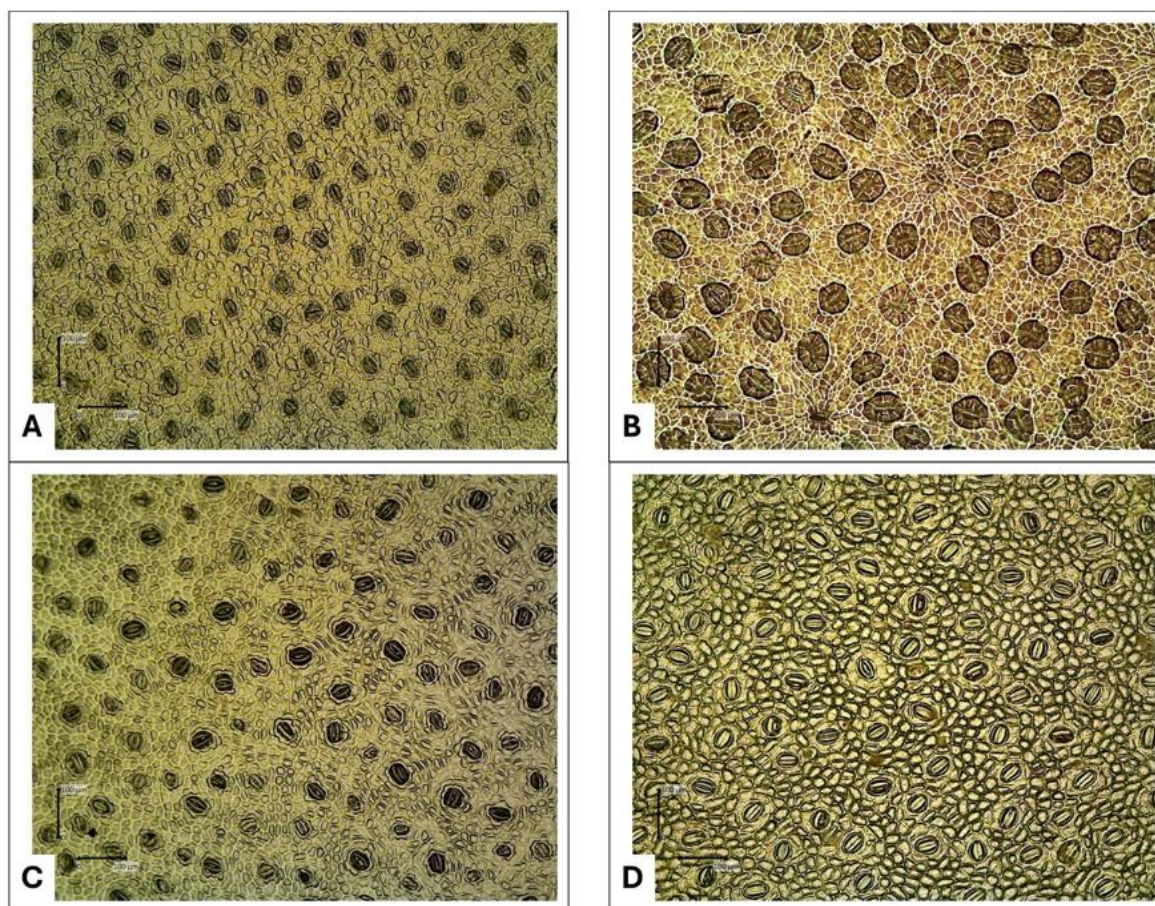


Figure 5. Stomatal replica of Rhizophoraceae mangrove in Benoa Bay (A) *Bruguiera gymnorhiza*; (B) *Ceriops tagal*; (C) *Rhizophora apiculata*; and (D) *Rhizophora mucronata*.

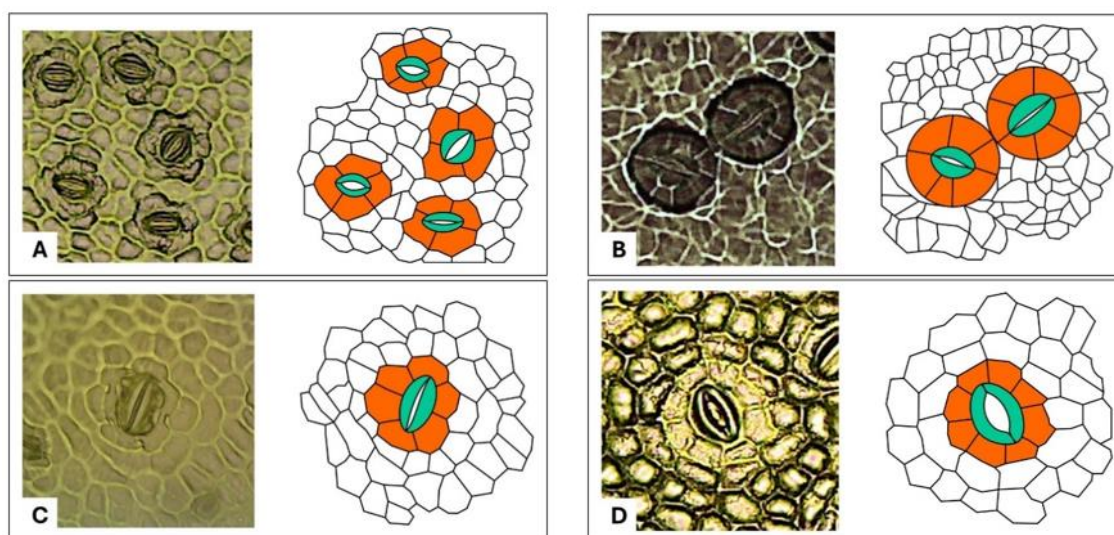


Figure 6. Stomatal illustration of Rhizophoraceae mangrove in Benoa Bay (A) tetracytic in *Bruguiera gymnorhiza*; (B) cyclocytic in *Ceriops tagal*; (C) anomocytic in *Rhizophora apiculata*; and (D) anomocytic in *Rhizophora mucronata*. The white cells represent the epidermal cells, the orange cells represent the subsidiary cells, and the green cells represent the guard cells.

Table 4. The leaf anatomical characteristics of Rhizophoraceae mangrove in each sampling site.

No	Characters	Species									
		BG-1	BG-2	BG-4	CT-1	CT-4	RA-1	RA-3	RM-1	RM-2	RM-3
Transversal section through the midrib											
1	Shapes of the vascular tissue	U-shaped	U-shaped	U-shaped	Rounded with U-shaped at the lower Present	Rounded with U-shaped at the lower Present	Rounded with U-shaped at the lower Present	Rounded with U-shaped at the lower Present	Rounded with U-shaped at the lower Present	Rounded with U-shaped at the lower Present	Rounded with U-shaped at the lower Present
2	Oxalate crystal in vascular tissue	Present	Present	Present	Present	Present	Present	Present	Present	Present	Present
3	Oxalate crystal in parenchyma tissue	Present	Present	Present	Present	Present	Present	Present	Present	Present	Present
4	Number of upper hypodermal layer(s) in the midrib	2-3	2-3	2-3	2-3	2-3	6-8	5-7	5-7	5-7	5-7
5	Occurrence of mesophyll palisade above the vascular tissue	Absent	Absent	Absent	Present	Present	Absent	Absent	Absent	Absent	Absent
6	Occurrence of sclereid (spheroidal) in vascular tissue	Yes, small amount	Yes, small amount	Yes, small amount	Yes, moderate amount	Yes, high amount	Yes, moderate amount	Yes, moderate amount	Yes, small amount	Yes, small amount	Yes, moderate amount
7	Occurrence of sclereid (rhizosclereid) in palisade	Absent	Absent	Absent	Absent	Absent	Present	Present	Present	Present	Present
8	Occurrence of sclereid (astroclereid) in midrib parenchyma	Absent	Absent	Absent	Absent	Absent	Yes, small amount	Yes, small amount	Yes, small amount	Yes, high amount	Yes, high amount
Transversal section through the lamina											
9	Thickness of upper epidermal layer(s) (μm)	17.66 \pm 1.57	16.74 \pm 3.04	18.63 \pm 3.16	13.68 \pm 1.15	15.43 \pm 1.56	10.47 \pm 1.10	10.56 \pm 0.95	10.40 \pm 1.03	10.82 \pm 1.28	10.60 \pm 1.01

Table 4 (Continue). The leaf anatomical characteristics of Rhizophoraceae mangrove in each sampling site.

No	Characters	Species									
		BG-1	BG-2	BG-4	CT-1	CT-4	RA-1	RA-3	RM-1	RM-2	RM-3
10	Thickness of upper hypodermal layer(s) (μm)	20.56 \pm 3.40	26.74 \pm 3.64	29.00 \pm 3.38	56.38 \pm 6.15	56.85 \pm 8.74	234.55 \pm 25.30	305.44 \pm 32.32	226.81 \pm 47.03	255.87 \pm 25.26	197.72 \pm 22.24
11	Thickness of palisade layer(s) (μm)	144.76 \pm 25.81	101.16 \pm 6.93	176.64 \pm 16.86	71.84 \pm 14.27	94.80 \pm 8.23	98.05 \pm 16.50	127.77 \pm 16.38	103.61 \pm 15.74	116.18 \pm 16.21	92.93 \pm 13.84
12	Thickness of sponge layer(s) (μm)	330.21 \pm 55.99	371.58 \pm 66.94	307.54 \pm 42.82	323.25 \pm 43.12	377.29 \pm 28.42	200.38 \pm 26.51	210.52 \pm 17.59	221.88 \pm 21.20	219.35 \pm 27.55	241.79 \pm 45.59
13	Thickness of lower hypodermal layer(s) (μm)	15.29 \pm 3.03	16.63 \pm 1.45	16.68 \pm 2.15	49.40 \pm 7.75	60.32 \pm 4.05	21.33 \pm 3.33	23.13 \pm 3.59	19.83 \pm 3.31	15.67 \pm 2.60	20.46 \pm 2.57
14	Thickness of lower epidermal layer(s) (μm)	15.59 \pm 1.48	14.08 \pm 1.51	14.04 \pm 1.44	14.92 \pm 2.94	12.87 \pm 2.16	11.08 \pm 2.00	10.37 \pm 0.92	10.87 \pm 1.25	10.96 \pm 1.65	11.36 \pm 1.25
15	Number of upper hypodermal layer(s) (μm)	1	1	1	2	2	6-7	6-7	5-6	5-6	5-6
16	Number of lower hypodermal layer(s) (μm)	1	1	1	2	2	1	1	1	1	1
17	Upper hypodermal gradation	Absent	Absent	Absent	Absent	Absent	Present	Present	Present	Present	Present
18	Overlapping hypodermal to palisade	Absent	Absent	Absent	Absent	Absent	Present	Present	Present	Present	Present
19	Thickness ratio of upper hypodermal to lamina	0.04	0.05	0.05	0.11	0.09	0.41	0.44	0.38	0.41	0.34
20	Thickness ratio of mesophyll palisade to sponges	0.42	0.26	0.54	0.22	0.25	0.49	0.61	0.47	0.53	0.38

Table 4 (Continue). The leaf anatomical characteristics of Rhizophoraceae mangrove in each sampling site.

No	Characters	Species									
		BG-1	BG-2	BG-4	CT-1	CT-4	RA-1	RA-3	RM-1	RM-2	RM-3
21	Thickness ratio of mesophyll palisade to lamina	0.27	0.18	0.31	0.14	0.15	0.17	0.19	0.17	0.18	0.16
22	Thickness ratio of mesophyll sponges to lamina	0.64	0.71	0.58	0.61	0.61	0.35	0.31	0.37	0.35	0.42
23	Oxalate crystal in hypodermal	Present	Present	Present	Present	Present	Present	Present	Present	Present	Present
24	Oxalate crystal in palisade	Present	Present	Present	Present	Present	Absent	Absent	Absent	Absent	Absent
25	Oxalate crystal in sponges	Present	Present	Present	Present	Present	Present	Present	Present	Present	Present
26	Occurrence of sclereid (rhizosclereid) in palisade	Absent	Absent	Absent	Absent	Absent	Absent	Present, small amount	Present, high amount	Present, high amount	Present, high amount
27	Occurrence of sclereid (astrosclereid) in sponges	Absent	Absent	Absent	Absent	Absent	Present	Present	Present	Present	Present
Replica paradermal											
28	Type of stomata	Tetracytic	Tetracytic	Tetracytic	Cyclocyctic	Cyclocyctic	Anomocytic	Anomocytic	Anomocytic	Anomocytic	Anomocytic
29	Index of stomata (IS) (%)	6.16 ± 0.48	5.17 ± 0.47	5.37 ± 0.25	4.15 ± 0.55	3.05 ± 0.50	3.69 ± 0.22	3.98 ± 0.34	4.27 ± 0.18	6.67 ± 0.22	5.21 ± 0.13
30	Density of stomata (mm ⁻²)	115.33 ± 8.08	140.33 ± 8.74	100.33 ± 2.08	65.33 ± 7.23	68.67 ± 8.08	80.00 ± 4.36	88.67 ± 4.93	84.77 ± 17.19	105.00 ± 7.55	72.33 ± 8.62
31	Density of epidermal cells (mm ⁻²)	1765.33 ± 224.13	1916.67 ± 63.50	1769.33 ± 57.55	1521.00 ± 236.58	2196.67 ± 154.57	2086.33 ± 17.90	2145.67 ± 77.22	1890.57 ± 297.13	1469.00 ± 64.13	1313.67 ± 128.25

Based on the results obtained, differences in environmental conditions do not indicate any change in qualitative character. This shows that each species has consistent qualitative characteristics, such as the vascular bundle, the number of hypodermis layers, the presence of sclereids, and the type of stomata. However, there are several differences in quantitative characters, such as tissue thickness which indicate the adaptation mechanisms to the environment. This is in line with the research results of [Tobing et al. \(2022\)](#) which states that *Avicennia marina* in areas with differences in salinity does not show differences in qualitative characters, but there are histological modifications that cause differences in tissue thickness. Variations in tissue thickness of leaves can be caused by various things, but the two main factors are fluctuations in salinity and water deficit which cause the formation of histological modifications to provide higher efficiency in cooling leaf temperature through convection and reduce the rate of water loss ([Sánchez et al., 2021](#); [Tatongjai et al., 2021](#)).

In adult individuals, anatomical characters tend to have adapted to fluctuations in environmental fluctuations. Thus, they have more consistent patterns than juveniles ([Sánchez et al., 2021](#); [Strock et al., 2022](#)). In epidermal tissue, all species have one layer of epidermis with a thick cuticle. The cuticle is a derivative of the epidermis in the form of a wax layer that is secreted on the surface of the tissue as a hydrophobic barrier to protect against sunlight while reducing the occurrence of non-stomatic water loss due to perspiration ([Chorchuhirun et al., 2020](#); [Sánchez et al., 2021](#)). Apart from the cuticle, the upper and lower epidermis also have derivatives in the form of hypodermis tissue. The upper hypodermis tissue tends to develop better than the lower hypodermis. The comparison of cell shape and size between the upper epidermis and upper hypodermis is also very significant, where epidermal cells are smaller compared to the hypodermis.

The hypodermis is a differentiated structure to prevent excessive water loss. Thus, it is commonly found in plants adapted to high-light-intensity stress ([Chorchuhirun et al., 2020](#)). In mangroves, the hypodermis tends to have thicker cell walls. Thickening of the hypodermis is a response to water deficit due to salinity, where the need to accumulate water causes plants to increase storage tissue through the formation of elongated hyaline cells, making it possible to overcome water deficit and withstand osmotic shock through the accumulation of solutes in the vacuoles of these cells ([Sánchez et al., 2021](#)). In addition, the hypodermis layer can play a role in filtering sunlight during the photosynthesis process. Thus, the energy in the sun is in optimal conditions for use by photosynthetic tissue. Based on the study, the *Rhizophora* genus has a very thick upper hypodermis, even reaching 7 layers in RM and 8 layers in RA. Other genera such as BG only have 1 layer, while CT has 2 layers of hypodermis.

Under the hypodermis, there are two mesophyll tissues commonly found in dicotyledonous plants, mesophyll palisade and sponge. Even though they have the same tissue, there are several distinct variations. The palisade tissue is shaped like a pillar with a very dense arrangement as salinity and light intensity increase ([Sánchez et al., 2021](#); [Tobing et al., 2022](#)). [Tobing et al. \(2022\)](#) found out that the palisade tissue of *A. marina* leaves that live on the coast is thicker than those in the pond with lower salinity. Even though they are different species, BG and CT which are adapted to environments with low salinity have lower palisade densities compared to RM and RA which are adapted to environments with higher salinity. Because the palisade density is very high, cells in the palisade mesophyll in RA and RM are very difficult to distinguish.

The mesophyll sponge tissue is located just below the palisade tissue. The characteristics of this tissue are also influenced by salinity and light intensity. Thus, it shows relatively the same adaptation pattern as palisade tissue ([Parida et al., 2004](#); [Sánchez et al., 2021](#); [Tatongjai et al., 2021](#); [Tobing et al., 2022](#)). The shape of sponge cells tends to be the same

which is rounded to irregular with slight variations in the size of the air chamber. The size of this air chamber is relatively narrow when compared to leaves of common dicotyledonous due to its relation to their adaptation to environmental stress. [Sánchez et al. \(2021\)](#) stated that under high light intensity and salinity stress, chloroplast efficiency tends to decrease then increasing the density of palisade tissue to overcome this, while on the other hand, there is a thickening of the sponge tissue with a reduction in the space between cells to reduce water loss during the stomata opening process. This shows that there is a high sensitivity of palisade and sponge tissue to environmental conditions. Thus, it can be used as an indicator of environmental change ([Parida et al., 2004](#); [Carriquí et al., 2021](#); [Khan et al., 2022](#)).

In carrying out their function as assimilation tissue, palisade, and sponges tissue need vascular bundles to circulate water, minerals, and the assimilation products. The vascular bundle in these mangrove leaves consists of a xylem and phloem with varying arrangements. There are two major arrangements of vascular bundle based on the results, one is U-shaped as in BG, and the other is rounded with U-shaped at the lower in CT, RA, and RM. The U shape of the BG resembles a crescent shape, which can also be found in other mangrove species such as *B. cylindrica* and *B. sexangula* ([Surya & Hari, 2016](#)). It is also known as the common shape of vascular bundles in mangrove species ([Tihurua et al., 2023](#)). Meanwhile, on CT, RA, and RM, the initial shape is thought to resemble a circular bicollateral pattern, and then there is an addition like a crescent shape at the bottom. This determination is based on the position of the xylem which is generally located in the middle.

Around the vascular bundles, there is an ergastic substance in the form of calcium oxalate crystals which are the remains of plant metabolism. The vascular bundles surrounded by calcium oxalate crystals aim to regulate calcium metabolism while avoiding excessive deposition in the assimilation parenchyma which can disrupt cellular function ([Tatongjai et al., 2021](#)). Related to the taxonomical study, the shape and chemical composition of calcium oxalate crystals are known as primary additional taxonomic markers to solve the taxonomic uncertainties in several taxa ([Raeski et al., 2023](#)). In this study, the calcium oxalate crystals were only in the form of a drusen crystal in a distinctive cell as typical idioblasts. These calcium oxalate crystals are not only scattered all over the vascular bundles, but also in the hypodermis, palisade, and sponge tissue. In conjunction with calcium oxalate crystals, sclereid cells are also scattered in various plant tissues.

Sclereids provide mechanical support to plant tissue and also play a role in reducing turgor pressure and deterring herbivory ([Vinoth et al., 2019](#); [Tatongjai et al., 2021](#)). There are three types of sclereids in the four mangrove species of the Rhizophoraceae: spheroidal sclereid, rhizosclereid, and astrosclereid. Spheroidal sclereids are monomorphic sclereids that are distributed around the vascular bundles, precisely on the outside of the phloem, to strengthen and protect the vascular bundles. The other two sclereids are rhizosclereid and astrosclereid which are classified as polymorphic sclereids. Rhizosclereids are only found in RA and RM which are distributed in the palisade mesophyll tissue. At first glance, the sclereids found in the palisade tissue resemble palosclereid, a sclereid with a pole shape that is parallel to the palisade cells ([Rao & Bhupal, 1973](#)). However, the tip of the observed sclereid has long branches that reach the spongy tissue which is more resemblance the rhizosclereid as described by [Richter \(1920\)](#). Another sclereid is the astrosclereid which is found in the sponge mesophyll and parenchyma tissue in the midrib. Astrosclereids commonly are found in tissue with big air chambers, because they play a role in providing mechanical support to increase strength in soft tissue ([Tatongjai et al., 2021](#)), therefore they are dominantly found in spongy tissue. Based on [Rao & Bhupal \(1973\)](#), there are four types

of astrosclereids: a typical astrosclereids with a star shape, ophiurosclereid with long and irregular arms, librosclereid with two arms that are longer than the other two or three arms, and trichosclereid with four long arms and thickening in the middle. Thus, they have a shape like the letter "H".

Other characteristics that can be observed are from the paradermal replica of the lower epidermis which consists of stomata type, index of stomata, density of stomata, and density of epidermal. Stomata type determination is based on the presence of subsidiary cells around the guard cells to the epidermal cells. This trait has its uniqueness in particular taxa and has become one of the considered traits to solve taxonomic uncertainties (Hong *et al.*, 2018; Gul *et al.*, 2019; Dubberstein *et al.*, 2021; Tihuraa *et al.*, 2023). In this study, there were three types of stomata: the tetracytic type in BG, the cyclocytic type in CT, and the anomocytic type in RA and RM. The tetracytic type is stomata with four subsidiary cells. The cyclocytic type is stomata with subsidiary cells surrounding the guard cells, and the shape of the subsidiary cells is different from epidermal cells. In RA and RM, it appears that subsidiary cells also surround the guard cells. Thus, some researchers classify them as cyclocytic types (Vinoth *et al.*, 2019). However, in this study, although it appears that subsidiary cells surround guard cells, the shape of these subsidiary cells is relatively similar to the shape of epidermal cells and their number tends not to be constant. Based on this, the type of stomata in RA and RM is classified as anomocytic type defined as stomata with the shape of subsidiary cells that are relatively similar to epidermal cells. Tihuraa *et al.* (2020) also classified the stomata type of RA as anomocytic.

While the type of stomata is a qualitative character, the index of stomata (IS), density of stomata, and density of epidermal are quantitative characters that tend to be sensitive to environmental fluctuations (Zhu *et al.*, 2018). The stomatal index in RA has the lowest variation with $3.69 \pm 0.22\%$ to $3.98 \pm 0.34\%$, while the others have a difference range of up to 1% in BG and CT, even reaching 2% in RM. In general, the IS in mangroves has a much lower value compared to other plants. In this study, the highest IS was in RM-2 ($6.67 \pm 0.22\%$) and the lowest was in CT-2 ($3.05 \pm 0.50\%$). In comparison to other plants, eleven species in *Indigofera* has IS ranged 9.95-27.46%, 43 genotypes of *Coffea canephora* have IS that ranged from 20.00-27.90% (Dubberstein *et al.*, 2021), some species from Sterculiaceae and Verbenaceae has IS ranged 15.85-22.31% (Ajuziogu *et al.*, 2018), 22 Lamiaceae species in the adaxial surface has IS ranged 10.6-57.42% (Gul *et al.*, 2019), and even in some fern species of Athyriaceae and Pteridaceae has IS ranged 8.0-23.07% (Shah *et al.*, 2018, 2019).

Overall, the anatomy of Rhizophoraceae leaves resembles typical dicotyledonous leaves, consisting of epidermal tissue, mesophyll palisade, mesophyll sponges, vascular bundles, and stomata. However, there are several particular structures found, such as the hypodermis layer, astrosclereids, and calcium oxalate crystals. Those structures show adaptation to environmental conditions. BG and CT have landward habitats. Thus, the hypodermis layer is thinner and the mesophyll tissue is not too dense. This is different from RA and RM which are adapted to seaward environments. Thus, its have thicker hypodermis, denser mesophyll, and the presence of astrosclereids to strengthen the leaves. All species have low IS, indicating structural adaptation for gas exchanges in unfavorable environments.

3.2. Taxonomic Significance of The Leaf Anatomical Characteristics of Rhizophoraceae Mangrove

The 21 selected data that have been scored are then subjected to cluster analysis and a dendrogram is constructed as an initial screening to determine its congruence to the prior taxonomic data (Figure 7). From these data, the result shows corresponding clustering with

morphology-based taxonomic data. BG group together to form their cluster, the same as CT. These two species form a larger cluster at a similarity of 0.66. On the other hand, RM and RA also form their cluster and the two species combine at a similarity of 0.80. The BG-CT cluster complex then merged with the RM-RA complex at a similarity of 0.31.

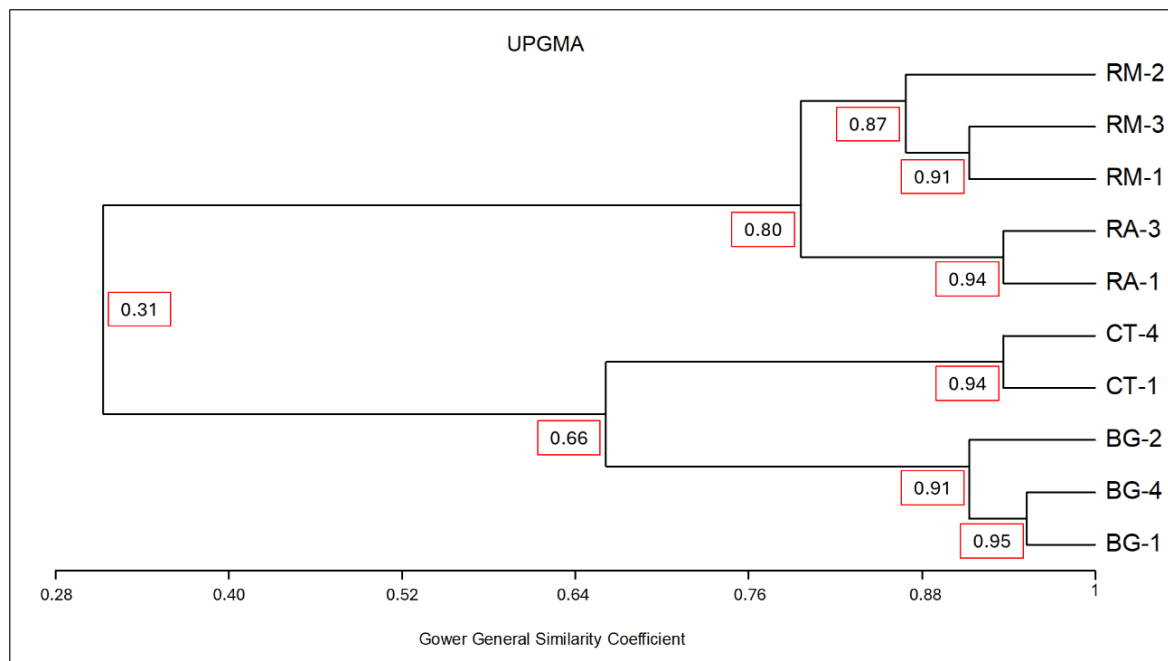
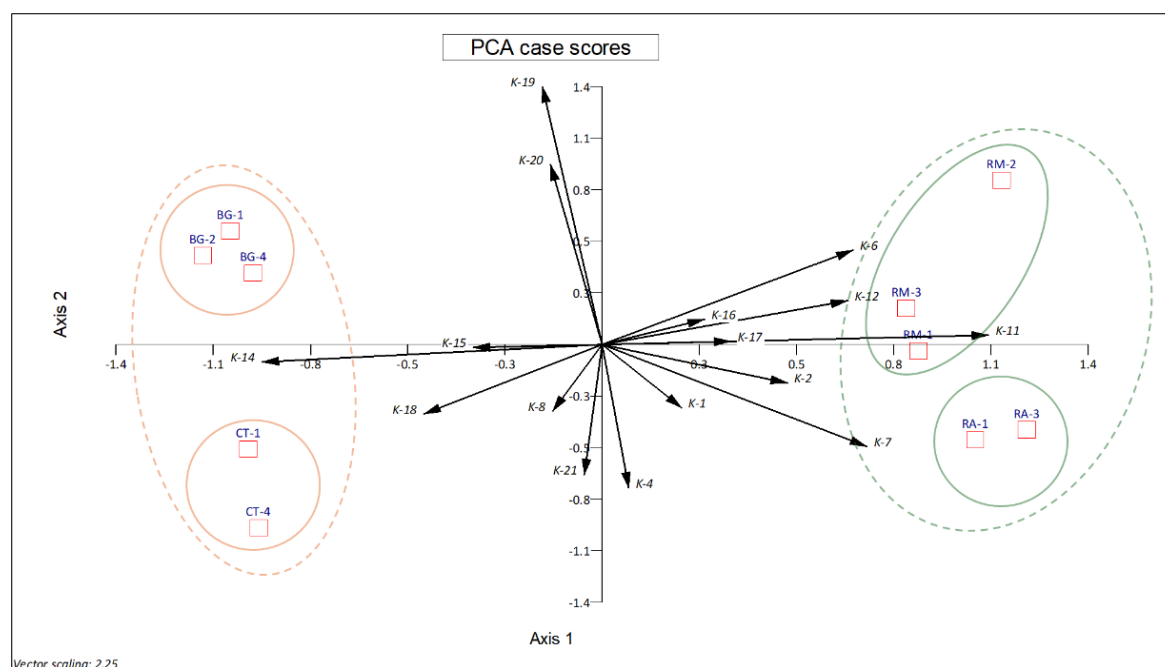


Figure 7. Dendrogram of Rhizophoraceae mangrove in Benoa Bay based on anatomical characteristics.

To study the characters that play a role in forming these clusters, principal component analysis (PCA) is carried out with eigenvalues for nine axes that are shown in **Table 5**. To evaluate the PCA representativeness towards the data, the cumulative percentage of the variations in the three main axes was evaluated. The most favorable situation in PCA is if the first three axes contain 80% or more of the total variations, hence it became the benchmark for the accuracy in PCA. In this study, the first three axes have a cumulative percentage of 94.40% (Axis 1 = 65.63%; Axis 2 = 20.14%; Axis 3 = 8.64%) that shows the PCA's data is appropriate because it indirectly implies most of the variations have been explained in those axes. To visualize the PCA, the scatter plot for Axis 1 and 2 (85.77% cumulative percentage variations) was generated as shown in **Figure 8**. If the PCA's scatter plot is linked to the dendrogram, BG and CT are on opposite sides with RM and RA as in dendrograms which represent different clusters. As axis 1 (65.63%) represents percentage variations three times higher than axis 2 (20.14%), the characters that are close to axis 1 are prioritized. The two main characters who play a role in this separation are K-11 and K-14. K-11 is the "thickness ratio of hypodermal to lamina" which has the highest value in RM and RA while the lowest in BG and CT. This character causes RM and RA to be on the right side. On the other hand, K-14 is the "thickness ratio of mesophyll sponges to lamina" with the highest values in BG and CT and the lowest in RM and RA. This character causes BG and CT to be on opposite sides of RM and RA.

Table 5. Eigenvalues and cumulative percentage of principal component analysis (PCA) of Rhizophoraceae mangrove in Benoa Bay based on anatomical characteristics.

Parameter	Axis 1	Axis 2	Axis 3	Axis 4	Axis 5	Axis 6	Axis 7	Axis 8	Axis 9
Eigenvalues	10.60	3.25	1.40	0.44	0.19	0.12	0.09	0.05	0.01
Percentage	65.63	20.14	8.64	2.71	1.20	0.76	0.55	0.30	0.08
Cum. Percentage	65.63	85.77	94.40	97.11	98.31	99.07	99.62	99.92	100.00

**Figure 8.** Scatter plot of principal component analysis (PCA) of Rhizophoraceae mangrove in Benoa Bay based on anatomical characteristics.

Other characters that give rise to polarity are K-6, K-7, K-12, and K-18. K-6 is the "occurrence of sclereid (astrosclereid) in midrib parenchyma" which shows the maximum value in RM followed by RA. Thus, it points to the right of the RM quadrant. This pattern is the same as the pattern in K-12, namely "thickness ratio of mesophyll palisade to sponges" with high values in RM and RA. The same thing also happens to K-7 which is the maximum "number of upper hypodermal layer(s)" in RA, followed by RM and CT. In contrast to K-6 and K-12, the vector in K-7 points to the RA quadrant because it has the highest value. The opposite pattern is shown in K-18 which is the "type of stomata". RM and RA have the anomocytic stomata type with the lowest score, while BG has the tetracytic type with a higher score and CT has the cyclocytic type with the highest score. Because of this score, this pattern is inversely proportional to the previous pattern, which is the vector points to the left side in BG and CT.

Data from PCA revealed that several tissue characters had distinctive variations, including hypodermis, palisade, sponges, sclereids, and stomata types. The value of each character is presented in **Table 4**. In adapting to environmental stress, the hypodermis layer certainly has a very important role. Hypodermis with many layers is found in RA (6-7 layers) followed by RM (5-6 layers), CT (2 layers), and BG (1 layer). The more layers of the hypodermis, the thicker the hypodermis tissue is. This is directly in concordance with the ratio of hypodermis to leaf lamina. The lowest ratio was owned by BG (0.04-0.05) which had the thinnest hypodermis layer, while the highest ratio was in RA (0.41-0.44) which had the thickest

hypodermis. The thickness of the hypodermis is closely related to salinity. Thus, it is indirectly related to the zone of the mangrove species. Mangroves adapted to the seaward zone have a higher hypodermis-to-lamina ratio than those adapted to the landward zone (Tihuraa et al., 2020). Although the hypodermis layer in the study is very distinctive, the same species in different locations has variations in the hypodermis layer. Research by Rashid et al. (2020) in Bangladesh shows that RM only has 2 layers of hypodermis, while RA has 2-3 layers of hypodermis. The opposite happened to BG with 1 layer in this research and 6-7 layers in the results of research from Kerala, India (Surya & Hari, 2016). For some recorded hypodermal layers in RM, Phandee et al. (2019) observed 5-6 layers which is the same amount of layers as this research, while Rashid et al. (2020) found only 2 hypodermis layers. These results follow Tihuraa et al. (2023) which stated that the number of hypodermis layers in Rhizophoraceae might depend on the environment.

Apart from the hypodermis, the mesophyll sponges are also a tissue with relatively high character significance. The influence of the ratio of sponge mesophyll to leaf lamina on the PCA scatter plot shows that this assimilation tissue is the tissue that is sacrificed for the increase in hypodermis tissue. In other words, species with thick hypodermis tissue will have thinner spongy mesophyll, and conversely, those with thin hypodermis will have thicker spongy mesophyll. The impact is that the ratio of sponge mesophyll to lamina will be low in species with thick hypodermis tissue and higher in thinner hypodermis: RA (0.31-0.35), RM (0.35-0.42), CT (0.61), and BG (0.58-0.71).

Other characteristics that play a role in PCA grouping are the type of stomata and the presence of astrosclereid. For stomatal types, grouping is based on the characteristics of each genus. All *Rhizophora* genera have anomocytic type, *Bruguiera* has tetracytic, and *Ceriops* has cyclocytic type. This impacted the groupings based on this qualitative data to provide a clear polarity. As stated by Tihuraa et al. (2023), stomata and other epidermal structures have taxonomic significance in taxon identification. This also occurs in the astrosclereid presence in the parenchymal tissue of the midrib. BG and CT do not have this astrosclereid component, whereas RA has astrosclereids in small quantities and is more abundant in RM.

Qualitative characters tend to be stable, in contrast to quantitative characters which tend to be easily influenced by environmental conditions. Quantitative data from measurements such as tissue thickness ratio, index of stomata, density of stomata, and density of epidermal cell show differences within species. To ensure whether the differences were significant or not, a Mann-Whitney nonparametric analysis was carried out to compare the mean value on seven quantitative characters within species as shown in **Table 6**. Based on that, the characters K-12 (thickness ratio of mesophyll palisade to sponges) and K-13 (thickness ratio of mesophyll palisade to lamina) are the most plastic characters, because almost all species have significant differences in average values (except in the comparison of "RM-1 and RM-2"). The opposite happens in K-20 (density of stomata) which tends to show character stability, because only the pairs "BG-1 and BG-2" and "RM-2 and RM-3" show significant differences, while the other pairs show insignificant mean values.

Palisade and sponge mesophylls tend to have high plasticity. Thus, most of the K-12-K-14 characters have significantly different average values. Physiologically, a decrease in mesophyll thickness is related to an increase in stomata closure which results in a decrease in CO₂ conductivity. Thus, the phytochemical process in the leaf decreases (Parida et al., 2004). Mesophyll plasticity of mangrove in various conditions and habitats has also been reported in the species *B. parviflora* (Parida et al., 2004), *R. mucronata* (Phandee et al., 2019), *R. apiculata* and *B. cylindrica* (Tihuraa et al., 2020), *R. mucronata* (Perez et al., 2021),

S. caseolaris (Tatongjai *et al.*, 2021), *R. mangle* (Sánchez *et al.*, 2021), and also in *A. marina* (Tobing *et al.*, 2022). This plasticity is one of the flexibility of mangrove species in adapting to various local environmental conditions (Vinoth *et al.*, 2019). Thus, adjacent habitats with different environmental conditions will show variations in mesophyll. The same thing was also observed in the ratio of hypodermis to lamina, thus indicating a significant difference.

Table 6. The results of Mann-Whitney nonparametric analysis of the selected quantitative characters.

No	Paired samples	Characters						
		K-11	K-12	K-13	K-14	K-19	K-20	K-21
1	BG-1 and BG-2	(Sig. Diff.)	(Sig. Diff.)	(Sig. Diff.)	(Sig. Diff.)	(Sig. Diff.)	Insig.	Insig.
2	BG-1 and BG-4	(Sig. Diff.)	(Sig. Diff.)	(Sig. Diff.)	(Sig. Diff.)	Insig.	(Sig. Diff.)	Insig.
3	BG-2 and BG-4	Insig.	(Sig. Diff.)	(Sig. Diff.)	(Sig. Diff.)	Insig.	Insig.	Insig.
4	CT-1 and CT-4	(Sig. Diff.)	(Sig. Diff.)	(Sig. Diff.)	Insig.	(Sig. Diff.)	Insig.	(Sig. Diff.)
5	RA-1 and RA-3	(Sig. Diff.)	(Sig. Diff.)	(Sig. Diff.)	(Sig. Diff.)	Insig.	Insig.	Insig.
6	RM-1 and RM-2	(Sig. Diff.)	Insig.	Insig.	Insig.	(Sig. Diff.)	Insig.	(Sig. Diff.)
7	RM-1 and RM-3	Insig.	(Sig. Diff.)	(Sig. Diff.)	(Sig. Diff.)	(Sig. Diff.)	Insig.	(Sig. Diff.)
8	RM-2 and RM-3	(Sig. Diff.)	(Sig. Diff.)	(Sig. Diff.)	(Sig. Diff.)	(Sig. Diff.)	(Sig. Diff.)	Insig.

Annotations: (Sig. Diff.) = significantly different; Insig. = insignificant.

If the data are compared within species, the BG-1 which is in the pristine area has significant mean differences in K-11-K-14 towards BG-2 and BG-4 which is in a disturbed area. The same pattern was also observed between RA-1 towards RA-3 with significant differences in K-11-K-14 and insignificant in K-19-K-21. CT-1 and CT-4 have slightly different patterns with insignificant mean in K-14 and K-20. The most random pattern is in RM-1 towards RM-2 and RM-3. RM-1 and RM-2 show many insignificant values, but RM-1 and RM-3 show many significant values. While the RM-2 and RM-3 show the most significant value with only one insignificant value for K-21.

Of the various characters obtained in the lower epidermis of mangrove leaves, the stomata type has high taxonomic significance as shown by the PCA results. Other characteristics such as index of stomata (K-19), density of stomata (K-20), and density of epidermal cell (K-21) tend to vary. Based on the Mann-Whitney test, the comparison of the K-19-K-21 values in BG-2 and BG-4 shows an insignificant value. Due to both samples being retrieved from disturbed areas, this indirectly shows that the character of K-19-K21 in BG is relatively plastic between pristine areas and disturbed areas.

The opposite was found in the comparison of RA-1 with RA-3. These pristine and disturbed locations have insignificant K-19-K21 values, which indirectly indicate a stable character in different environments. In the pair of CT and RM, the K-19-K21 values tend to be irregular, that is some are significant, and some are not. However, one clear thing is that the index of stomata is significantly different in each pair on CT and RM. The index of stomata is the proportion of the number of stomata to the total cells in the epidermis. As the stomata responsible for the water-gas exchange mechanism, these variations can imply the stomatal adjustment in the local environment due to water-gas regulation (Zhu *et al.*,

2018; Khan et al., 2022). The plasticity also occurs in the density of stomata and epidermal cells, which is indirectly correlated with the index of stomata (Zhu et al., 2018). High photosynthesis and respiration rates will respond by increasing stomatal formation to balance water-gas exchange, hence the stomata density will increase along with decreasing in epidermal cell density (Niu et al., 2020). Plasticity in the density of stomata for this study did not bring many significant differences among pairs. Although the range of density of stomata in RA is 80.00-88.67 mm⁻², this value was not much different than the results of Tihurua et al. (2020) who obtained the RA's stomata density in Banggai (Sulawesi) in the range of 50.60-82.91 mm⁻².

Based on the overall data from the numerical taxonomic analysis, the grouping of species based on leaf anatomical characters in the dendrogram followed the applicable classification. This confirms the structural expression due to adaptation in a particular environment. From the PCA data, it is known that several characters have significant taxonomic implications, such as the thickness ratio of hypodermis to lamina, the thickness ratio of mesophyll sponges to lamina, the thickness ratio of palisade to sponges, the occurrence of astrosclereids, the number of hypodermal layers, and the type of stomata. The results of the Mann-Whitney nonparametric test indicating the quantitative characters (the tissue ratio and stomata) have the potential to be used as indicators of in assessing environmental conditions.

4. CONCLUSION

The anatomical structure of the leaves in *Bruguiera gymnorhiza*, *Ceriops tagal*, *Rhizophora apiculata*, and *Rhizophora mucronata* shows distinctive characteristics following their adaptation to the habitat in a stressed environment. Anatomical characters with taxonomic significance are found in the tissue structure of the hypodermis, mesophyll (palisade and sponges), distribution of calcium oxalate crystals, sclereids (particularly astrosclereids and rhizosclereids), and stomata. This structure is closely related to the natural zoning of mangroves, which is *B. gymnorhiza* and *C. tagal* preferred in the landward zone, while *R. apiculata* and *R. mucronata* are adapted from the landward to the seaward. Then, the conservation planning needs to consider the natural habitat of these mangrove species due to their adaptation. The same species with different habitat conditions show significant variations in the quantitative characteristics of the tissues, such as the thickness ratio of hypodermis to the lamina, the thickness ratio of mesophyll sponges to lamina, the thickness ratio of palisade to sponges, and the index of stomata. This variation shows plastic adaptation related to a change in environmental conditions that is responded to structurally. In further study, these plastic characteristics (especially mesophyll and hypodermis) can be used as indicators of climate change.

5. ACKNOWLEDGEMENTS

We thank the Research and Community Center, Udayana University, for funding resources through the Flagship Study Program research grant of PNPB number B/1.473/UN14.4.A/PT.01.03/2023. Many thanks also to the Biology Program and Faculty of Mathematics and Natural Sciences for the support and assistance on this project.

6. AUTHORS' NOTE

The author(s) declare(s) that there is no conflict of interest regarding the publication of this article. The authors confirmed that the data and the paper are free of plagiarism.

7. REFERENCES

- Adame, M.F., Connolly, R.M., Turschwell, M.P., Lovelock, C.E., Fatoyinbo, T., Lagomasino, D., Goldberg, L.A., Holdorf, J., Friess, D.A., Sasmito, S.D., Sanderman, J., Sievers, M., Buelow, C., Kauffman, J.B., Bryan-Brown, D., and Brown, C.J. (2021). Future carbon emissions from global mangrove forest loss. *Global Change Biology*, 27, 2856–2866.
- Ajuziogu, G.C., Ejeagba, P.O., Nwafor, F.I., Ayogu, V.O., Nweze, A.E., Asuzu, C.U., and Egonu, S.N.. (2018). Comparative anatomical studies of the stomatal patterns of some tree species of Sterculiaceae and Verbenaceae in Nigeria. *Pakistan Journal of Botany*, 50(2), 679–684.
- Andiani, A.A.E., Karang, I.W.G.A., Putra, I.N.G., and Dharmawan, I.W.E. (2021). Relationship among mangrove stand structure parameters in estimating the community scale of aboveground carbon stock. *Jurnal Ilmu dan Teknologi Kelautan Tropis*, 13(3), 485–498.
- Carriquí, M., Nadal, M., and Flexas, J. (2021). Acclimation of mesophyll conductance and anatomy to light during leaf aging in *Arabidopsis thaliana*. *Physiologia Plantarum*, 172(4), 1894–1907.
- Carugati, L., Gatto, B., Rastelli, E., Lo Martire, M., Coral, C., Greco, S., and Danovaro, R. (2018). Impact of mangrove forests degradation on biodiversity and ecosystem functioning. *Scientific Reports*, 8(13298), 1–11.
- Chorchuhirun, B., Kraichak, E., and Kermanee, P. (2020). Comparative anatomy of two mangrove species: *Xylocarpus granatum* and *Xylocarpus moluccensis* (Meliaceae). *Thai Journal of Science and Technology*, 9(3), 355–367.
- Dewi, I.G.A.I.P., Faiqoh, E., As-syakur, A.R., and Dharmawan, I.W.E. (2021). Natural regeneration of mangrove seedlings in Benoa Bay, Bali. *Jurnal Ilmu dan Teknologi Kelautan Tropis*, 13(3), 395–410.
- Dubberstein, D., Oliveira, M.G., Aoyama, E.M., Guilhen, J.H., Ferreira, A., Marques, I., Ramalho, J.C., and Partelli, F.L. (2021). Diversity of leaf stomatal traits among *Coffea canephora* Pierre ex A. Froehner genotypes. *Agronomy*, 11(6), 1126.
- Filartiga, A.L., Klimeš, A., Altman, J., Nobis, M.P., Crivellaro, A., Schweingruber, F., and Doležal, J. (2022). Comparative anatomy of leaf petioles in temperate trees and shrubs: the role of plant size, environment and phylogeny. *Annals of Botany*, 129(5), 567–582.
- Giri, C., Ochieng, E., Tieszen, L.L., Zhu, Z., Singh, A., Loveland, T., Masek, J., and Duke, N. (2011). Status and distribution of mangrove forests of the world using earth observation satellite data. *Global Ecology and Biogeography*, 20(1), 154–159.
- Gul, S., Ahmad, M., Zafar, M., Bahadur, S., Celep, F., Sultana, S., Begum, N., Hanif, U., Zaman, W., Shuaib, M., and Ayaz, A. (2019). Taxonomic significance of foliar epidermal morphology in Lamiaceae from Pakistan. *Microscopy Research and Technique*, 82(9), 1507–1528.
- Hong, T., Lin, H., and He, D. (2018). Characteristics and correlations of leaf stomata in different *Aleurites montana* provenances. *PLoS ONE*, 13(12), 1–10.
- Kauffman, J.B., Adame, M.F., Arifanti, V.B., Schile-Beers, L.M., Bernardino, A.F., Bhomia, R.K., Donato, D.C., Feller, I.C., Ferreira, T.O., Jesus Garcia, M.del C., MacKenzie, R.A.,

- Megonigal, J.P., Murdiyarto, D., Simpson, L., and Trejo, H.H. (2020). Total ecosystem carbon stocks of mangroves across broad global environmental and physical gradients. *Ecological Monographs*, 90(2), 1–18.
- Khan, A., Shen, F., Yang, L., Xing, W., and Clothier, B. (2022). Limited acclimation in leaf morphology and anatomy to experimental drought in temperate forest species. *Biology*, 11(8), 1–18.
- Lugina, M., Alviya, I., Indartik, and Pribadi, M.A. (2017). Sustainable strategy of mangrove management in Ngurah Rai Forest Park Bali. *Jurnal Analisis Kebijakan Kehutanan*, 14(1), 61–77.
- Marantika, M., Hiariej, A., and Sahertian, D.E. (2021). Density and distribution of leaf stomata in mangrove species in Desa Negeri Lama, Ambon. *Jurnal Ilmu Alam dan Lingkungan*, 12(1), 1-6.
- Niu, L., Yan, Y., Hou, P., Bai, W., Zhao, R., Wang, Y., Li, S., Dua, T., Zhao, M., Song, J., and Zhou, W. (2020). Influence of plastic film mulching and planting density on yield, leaf anatomy, and root characteristics of maize on the Loess Plateau. *Crop Journal*, 8(4), 548–564.
- Parida, A.K., Das, A.B., and Mittra, B. (2004). Effects of salt on growth, ion accumulation, photosynthesis and leaf anatomy of the mangrove, *Bruguiera parviflora*. *Trees*, 18, 167-174.
- Perez, K.L.D., Quimade, M.O., Maldia, L.S.J., Tinio, C.E., Hernandez, J.O., and Combalicer, M.S. (2021). Effects of copper on the leaf morpho-anatomy of *Rhizophora mucronata*: Implications for mangrove ecosystem restoration. *Biodiversitas*, 22(4), 2058-2065.
- Phandee, S., Soonthornkalump, S., and Buapet, P. (2019). Morphological and anatomical responses of the common mangrove *Rhizophora mucronata* seedlings to flooding. *Walailak Procedia*, 3, 1–9.
- Raeski, P.A., Ayres, G.D., Monteiro, L.M., Heiden, G., Novatski, A., Raman, V., Khan, I.A., Lourenço, E.L.B., Gasparotto, A., Farago, P.V., and Manfron, J. (2023). Applications of calcium oxalate crystal microscopy in the characterization of *Baccharis articulata*. *Brazilian Archives of Biology and Technology*, 66, e23230078.
- Raju, K.A., and Ramakrishna, C. (2021). The effects of heavy metals on the anatomical structures of *Avicennia marina* (Forssk.) Vierh. *Brazilian Journal of Botany*, 44(2), 439–447.
- Rao, T.A., and Bhupal, O.P. (1973). Typology of sclereids. *Proceedings of the Indian Academy of Sciences*, 77(2), 41–55.
- Rashid, P., Shethi, K.J., and Ahmed, A. (2020). Leaf anatomical adaptation of eighteen mangrove plant species from the Sundarbans in Bangladesh. *Bangladesh Journal of Botany*, 49(4), 903–911.
- Richter, A. (1920). Über einige I ewe Glie der Marcgravnaceen, auf Basie der phylogenie mad der Vergleichende Anatomie. *Math. Naturw. Bevichte Ungarn*, 31, 65–146.

- Romañach, S.S., DeAngelis, D.L., Koh, H.L., Li, Y., Teh, S.Y., Barizan, R.S.R., and Zhai, L. (2018). Conservation and restoration of mangroves: Global status, perspectives, and prognosis. *Ocean and Coastal Management*, 154, 72–82.
- Samiyarsih, S., Brata, T.S., and Juwano. (2016). Leaf anatomical characteristics of polluted mangrove in mangrove forest Cilacap Regency. *Biosfera*, 33(1), 31-36.
- Sánchez, A.R., Pineda, J.E.M., Casas, X.M., and Calderón, J.H.M. (2021). Influence of edaphic salinity on leaf morphoanatomical functional traits on juvenile and adult trees of red mangrove (*Rhizophora mangle*): Implications with relation to climate change. *Forests*, 12, 1586.
- Shah, S.N., Ahmad, M., Zafar, M., Razzaq, A., Malik, K., Rashid, N., Ullah, F., Iqbal, M., and Zaman, W. (2018). Foliar epidermal micromorphology and its taxonomic implications in some selected species of Athyriaceae. *Microscopy Research and Technique*, 81(8), 902–913.
- Shah, S.N., Celik, A., Ahmad, M., Ullah, F., Zaman, W., Zafar, M., Malik, K., Rashid, N., Iqbal, M., Sohail, A., and Bahadur, S. (2019). Leaf epidermal micromorphology and its implications in systematics of certain taxa of the fern family Pteridaceae from Northern Pakistan. *Microscopy Research and Technique*, 82(3), 317–332.
- Strock, C.F., Schneider, H.M., and Lynch, J.P. (2022). Anatomics: High-throughput phenotyping of plant anatomy. *Trends in Plant Science*, 27(6), 520–523.
- Sugiana, I.P., Andiani, A.A.E., Dewi, I.G.A.I.P., Karang, I.W.G.A., As-syakur, A.R., and Dharmawan, I.W.E. (2022). Spatial distribution of mangrove health index on three genera dominated zones in Benoa Bay, Bali, Indonesia. *Biodiversitas*, 23(7), 3407–3418.
- Surya, S., and Hari, N. (2016). Comparative study on foliar and petiole anatomy of the genus *Bruguiera* L. in mangrove forest of Kerala. *Journal of Academia and Industrial Research*, 5(7), 92–97.
- Tatongjai, S., Kraichak, E., and Kermanee, P. (2021). Comparative anatomy and salt management of *Sonneratia caseolaris* (L.) Engl. (Lythraceae) grown in saltwater and freshwater. *PeerJ*, 9, e10962.
- Thomas, N., Lucas, R., Bunting, P., Hardy, A., Rosenqvist, A., and Simard, M. (2017). Distribution and drivers of global mangrove forest change, 1996-2010. *PLoS ONE*, 12(6), 1–14.
- Tihurua, E.F., Agustiani, E.L., and Rahmawati, K. (2020). Character of leaf anatomy as form of plant adaptation on mangrove zonation in Banggai Islands, Central Celebes. *Jurnal Kelautan Tropis*, 23(2), 255–264.
- Tihurua, E.F., Rahmawati, K., Agustiani, E.L., Ardhiyani, M., Hutabarat, P.W.K., Nasution, T., Sutikno, Surya, D., Damayanto, I.P.G.P., Apandi, I., Dalimunthe, S.H., Martiansyah, I., and Junaedi, D.I. (2023). Leaf anatomical characters of several true mangrove species. *Berita Biologi*, 22(1), 11-128.
- Tobing, A.N.L., Darmanti, S., Hastuti, E.D., and Izzati, M. (2022). Anatomical adaptation of grey mangrove (*Avicennia marina*) leaf in the pond and coast located in Mangunharjo, Semarang, Central Java. *Biosaintifika*, 14(1), 57–64.

- Valiela, I., Bowen, J.I., and York, J.K. (2001). Mangrove forests: One of the world's threatened major tropical environments. *BioScience*, 51(10), 807–815.
- Vinoth, R., Kumaravel, S., and Ranganathan, R. (2019). Anatomical and physiological adaptation of mangrove wetlands in east coast of Tamil Nadu. *World of Scientific News*, 129, 161–179.
- Wijaya, I.M.S., Sugiana, I.P., Astarini, I.A., Ginantra, I.K., and Rahim, K.A.A. (2024). Floristic composition of mangrove community in Ngurah Rai Forest Park and Nusa Lembongan, Bali, Indonesia. *Biodiversitas*, 25(1), 300–309.
- Wijaya, I.M.S., Sugiana, I.P., Wijana, I.M.S., and As-Syakur, A.R. (2023). Comparison of mangrove vegetation in natural and ex-fisheries area in Benoa Bay, Bali. *AACL Bioflux* 16(2), 825–836.
- Zhu, J., Yu, Q., Xu, C., Li, J., and Qin, G. (2018). Rapid estimation of stomatal density and stomatal area of plant leaves based on object-oriented classification and its ecological trade-off strategy analysis. *Forests*, 9(10), 1–18.